Polym. Bull. (2011) 66:133–146
DOI 10.1007/s00289-010-0314-x

ORIGINAL PAPER

Microemulsion copolymerization of vinyl acetate and butyl acrylate using a mixture of anionic and non-ionic surfactants

Víctor M. Ovando-Medina · René D. Peralta · Eduardo Mendizábal · Hugo Martínez-Gutiérrez · Miguel A. Corona-Rivera

Received: 3 March 2010 / Revised: 27 May 2010 / Accepted: 30 May 2010 /
Published online: 6 June 2010

Abstract Monomer mixtures of vinyl acetate (VAc)/butyl acrylate (BuA) were polymerized in batch reactions at 60 °C with potassium persulfate as the initiator in microemulsions consisting of VAc:BuA (85:15 wt/wt)/water/sodium dodecyl sulfate (SDS)/polyoxyethylene (23) dodecyl ether (3:1 wt/wt). The effect of the concentration of the monomer mixture on the kinetics was studied. It was found that, as the total monomers concentration ($[M]_0$) increases, the polymerization rate increases also, and that the maximum polymerization rate is proportional to $[M]_0^{1.26}$. Particle size increases with total monomers concentration. In all cases, final average particle diameter was less than 50 nm. Particle number density is independent of total monomers concentration. A mathematical model that takes into account the partition of monomers between the different phases during polymerization using a minimum of adjustable parameters was applied to simulate the experimental data. A correlation for the radical desorption coefficient, which is a function of the rate of

V. M. Ovando-Medina (✉) · M. A. Corona-Rivera
Departamento de Ingeniería Química, COARA – Universidad Autónoma de San Luis Potosí, Carretera a Cedral Km 5+600, San José de las Trojes, 78700 Matehuala, SLP, México
e-mail: ovandomedina@yahoo.com.mx

R. D. Peralta
Centro de Investigación en Química Aplicada (CIQA), Blvd. Enrique Reyna 140, 25253 Saltillo, Coah, México

E. Mendizábal
Departamentos de Química y de Ingeniería Química, CUCEI, Universidad de Guadalajara, Blvd. Marcelino García Barragán 1451, 44430 Guadalajara, Jal, México

H. Martínez-Gutiérrez
Instituto Potosino de Investigación Científica y Tecnológica, Camino a la Presa San José 2055, 78216 San Luis Potosí, SLP, México

monomer chain transfer and of the probability of desorption, was used in the model. Radical capture by micelles and particles was assumed to occur by diffusion. The model takes into account both micellar and homogeneous nucleation. Good agreement between the model and the experimental results was observed.

Introduction

Microemulsion polymerization has gained importance in the last two decades, mainly due to the necessity to obtain water-based lattices containing particles with sizes smaller than those obtained by emulsion polymerization, which can have special applications. The homopolymers and copolymers of VAc are prepared in industry mainly by emulsion polymerization. Although there are no reports on the use of microemulsion polymerization in industrial applications yet, this method has some potential due to: a better control of particle size [1, 2], the nanometer-scale average particle sizes that are obtained [3], and because of these sizes, adhesive, mechanical, and physical properties of the films are improved [4]. However, a limitation to extend the industrial application of microemulsion polymerization for homopolymers and copolymers, in general, is the low ratio of polymer/surfactant in the final latex [5, 6]. Although VAc microemulsion polymerizations have been studied [7–9], there is a lack of reports on the microemulsion copolymerization of VAc with BuA, copolymers which are of industrial interest, e.g., in the coating, paint, and textile industries [10].

The purpose of this work is to study the characteristics of batch microemulsion copolymerization of the VAc/BuA system using a mixture of SDS/Brij-35 as emulsifier. Here, the mathematical model reported by Ovando-Medina et al. [11] was modified by replacing the adjustable parameters by correlations to calculate kinetic and transport parameters and used to simulate the microemulsion copolymerization of VAc with BuA. The model, as presented in this report, predicts the kinetic behavior of the microemulsion copolymerization of monomers with different water solubility such as the VAc/BuA system.

Experimental

Materials

Potassium persulfate (KPS), hydroquinone (HQ) and the non-ionic surfactant Brij-35 were purchased from Aldrich (>99%). VAc and BuA monomers from Aldrich were purified by washing them with an aqueous solution of NaOH (10 wt%). After washing, the monomers were dried with anhydrous magnesium sulfate for 12 h before distillation at reduced pressure at 35 and 50 °C, respectively, and stored at 4 °C. Water was deionized tridistilled grade obtained from a set of ionic interchange columns (Cole-Parmer Instruments Company) and the ultra-high purity argon was from Infra.

Experimental

The o/w microemulsion region for the VAc:BuA (85:15 wt/wt)/H_2O/SDS:Brij-35 (3:1 wt/wt) system at 60 °C was determined following the methodology reported elsewhere [12], which consists in the titration of mixtures of different surfactants/water ratios with the monomers mixture. The microemulsion boundaries were detected visually.

Polymerizations were carried out in a 250 mL glass reactor at 60 °C with magnetic stirring. Table 1 shows the recipes used in the polymerizations. The mixture of surfactants and water was charged to the reactor, cooled, vacuum degassed and saturated with argon, then the previously degassed monomers mixture saturated with argon was added to the reactor. The reaction mixture was heated to 60 °C and the KPS (2 wt% with respect to the monomer mixture) was charged to the reactor to initiate the polymerization. The reacting system was continuously stirred throughout the reaction and purged with argon each time that a sample was taken. Conversion was followed gravimetrically: samples were withdrawn from the reacting system at given times and poured into vials (of known weight) containing 0.5 g of an aqueous hydroquinone solution (0.4 wt%), which were immersed in an ice bath. Then, the vials were weighed and the water and the residual monomer were eliminated by freeze-drying using a Labconco Freeze Dry System/R45. The weight of polymer was estimated by subtracting the known weights of surfactants and hydroquinone from the total weight of the freeze-dried sample.

Characterization

Particle size was measured in a Malvern 4700 quasielastic-light-scattering (QLS) apparatus equipped with an argon laser ($\lambda = 488$ nm). Measurements were performed at 25 °C at an angle of 90°. Copolymer samples were washed with hot water (to remove surfactants), vacuum dried at 40 °C and then dissolved in chloroform and precipitated with anhydrous ethylic ether; finally, the polymer was vacuum dried for 24 h. Copolymer compositions were determined by ^{1}H-NMR in an FTNMR Gemini 200, Varian (200 MHz) apparatus, using 10 mg/mL sample solution in deuterated chloroform. Average molar masses and molar mass distributions (MMD) of copolymers were determined in a Hewlett-Packard series

Table 1 Recipes used in the batch microemulsion copolymerizations of VAc/BuA

Component (g)	$[M]_0$ (wt%)		
	2	3	4
H_2O	140.874	139.437	138.000
SDS	4.594	4.547	4.500
Brij-35	1.531	1.515	1.500
VAc	2.550	3.825	5.100
BuA	0.450	0.675	0.900
KPS	0.060	0.090	0.120

1100 gel permeation chromatograph equipped with a refractive index detector and using HPLC-grade tetrahydrofurane (Aldrich) as the mobile phase. Because polystyrene standards were used, the weighted averages of the parameters in the Mark–Houwink equation, α and K, were calculated using the cumulative copolymer composition (obtained previously by ^{1}H-NMR spectrometry) following the procedure reported by Jovanovic and Dubé [13] for correction of GPC results.

Results

To obtain a large microemulsion zone using a low surfactant concentration, a combination of ionic and non-ionic surfactant was used. In previous experiments, we tested five surfactant systems trying to find a combination of anionic and non-ionic surfactants that gave the widest microemulsion region while keeping a low proportion of these components. The mixture of SDS/Brij-35 (3:1 wt/wt) met the requirements.

Figure 1 shows the water-rich partial phase diagram of the pseudo-ternary VAc:BuA (85:15 wt/wt)/water/SDS:Brij-35 (3:1 wt/wt) system at 60 °C. The partial phase diagram reported here presents a larger microemulsion region at low surfactant/water ratios than that reported by Torres-Plata [14] for a similar system but using bis(2-ethylhexyl) sulfosuccinate (AOT) as the surfactant instead of Brij-35.

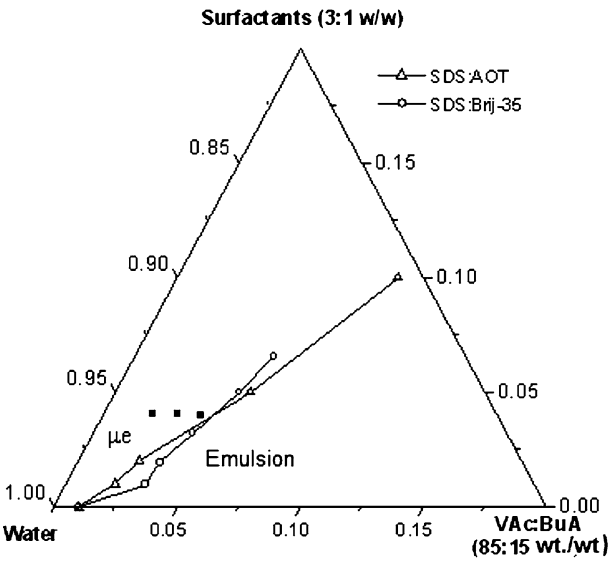

Fig. 1 Partial phase diagram at 60 °C in which the microemulsion (μe) and emulsion regions for the VAc:BuA (85:15 wt/wt)/H_2O/SDS:Brij-35 (3:1 wt/wt) system is presented. Data corresponding to the VAc:BuA (85:15 wt/wt)/H_2O/SDS:AOT (3:1 wt/wt) system were taken from Torres-Plata [14]. *Dark dots* correspond to compositions where polymerizations were made

It is known that the presence of a non-ionic surfactant results in a marked reduction of the critical micellar concentration (CMC) of the emulsifier mixture. This reduction in CMC is due to the intercalation of polar heads of the non-ionic groups between the polar heads of the anionic surfactant (sulfate) introducing enough separation among the sulfate groups so that any change in ionic strength has an effect on electrostatic interaction [15]. Donescu et al. [16] studied ternary microemulsions of vinylic and acrylic monomers. They found that hydrophobic monomers are solubilized toward the hydrocarbon interior of the micelles whereas the hydrophilic ones, toward the polar head of the surfactant. This localization of the hydrophobic monomers (water solubility of BuA $\approx$ 0.16% [17]) has a synergistic effect as a co-emulsifier, which increases with SDS concentration. The broadening of the microemulsion region at low surfactant concentrations could imply that the co-emulsifier effect of the BuA monomer is significant in this region and weakens when surfactant concentration is increased, particularly when Brij-35 content is increased.

Figure 2 shows a comparison between experimental results and model predictions of conversion versus time data as a function of the initial monomers concentration. High final conversions were obtained. Initially, clear microemulsions were obtained which turned bluish and translucent at the early stages of the reaction, and became less translucent towards the end of the polymerization. The latexes were very stable and no phase separation or precipitation was observed after 9 months of storage. Simulations were made using the modified model as detailed in the Appendix. Good agreement between experimental results and model predictions was obtained.

Figure 3 shows the experimental and simulated evolution of average particle size as a function of conversion for different monomers mixture concentrations. Both, experimental and calculated results show that particle size increases with increasing

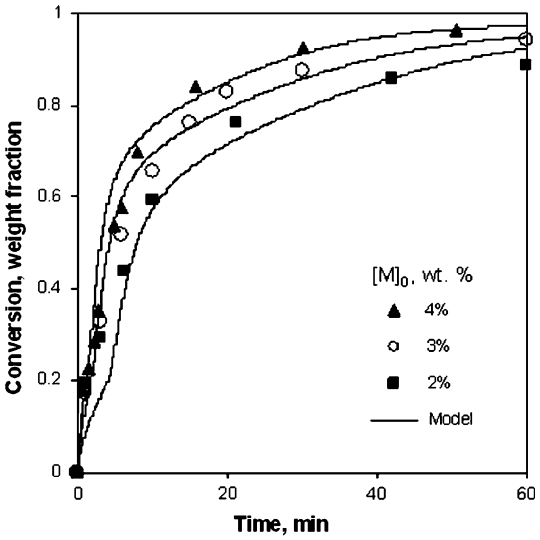

Fig. 2 Experimental and simulated conversion versus time plot for the batch microemulsion copolymerization of VAc:BuA (85:15 wt/wt) at 60 °C, 2 wt% of KPS with respect to the monomer content, 4 wt% of emulsifier mixture and different monomers mixture concentrations in the initial charge

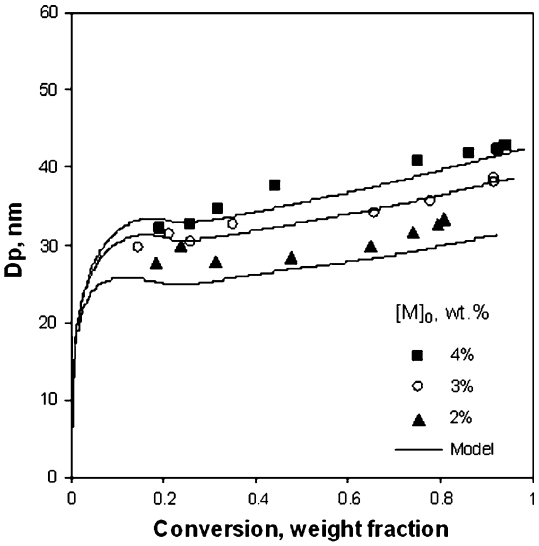

Fig. 3 Particle size versus conversion for the microemulsion copolymerization of VAc:BuA (85:15 wt/wt) at 60 °C, 2 wt% of KPS with respect to the monomer content for different monomers concentrations. *Dots* are experimental data and *continuous curves* are model predictions

conversion and monomers mixture concentration in the recipe. After the particle diameter grows to ~30 nm, simulation shows a slight decrease in particle size reaching a minimum value between 25 and 30% conversion and then it grows again. This minimum is related to particle formation by homogeneous nucleation, which is more evident because the reaction starts to be controlled by the VAc polymerization due to BuA depletion.

In Fig. 4, the experimental and simulated particles number density, N_p, as a function of conversion are shown. An increase in N_p with conversion can be observed. Equation 1 was used to calculate N_p [18]:

$$N_p = \frac{6[M]_0 X}{\pi D_{p_v}^3 \rho_p} \quad (1)$$

where N_p is the number density of particles, $[M]_0$ is the initial monomers concentration in the reactor, X is the conversion, D_{p_v} is the experimental average diameter of the particles (with the assumption that they are spherical and monodisperse) and ρ_p is the copolymer density. In Eq. 1, the z-average particle diameter obtained from QLS measurements was used.

As illustrated in Fig. 5, only two populations can be clearly seen (continuous curves) for the MWD at low conversions and the proportion of high molecular weight population decreases as conversion increases. To reveal hidden peaks in the experimental MWD, deconvolutions at different conversions were carried out with commercial software (Peak fit v4®, AISSN Software, Inc.) using Gaussian distributions. It was found that at low (19%) and until relatively high (84%) conversions, deconvolutions revealed three populations which collapsed into two towards the end of the copolymerization (94% conversion).

Figure 6 shows simulated results of copolymer composition versus global conversion for the microemulsion copolymerization of VAc/BuA (85:15 wt/wt)

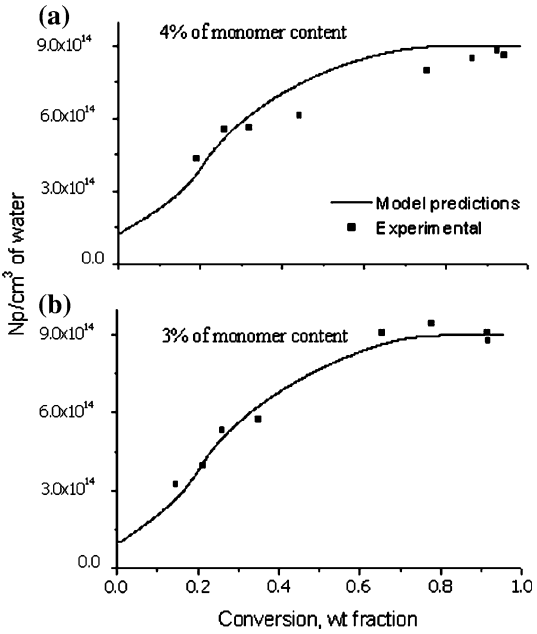

Fig. 4 Number of particles versus conversion for the microemulsion copolymerization of VAc:BuA (85:15 wt/wt) at 60 °C, 2 wt% of KPS with respect to the monomer content for different monomers concentrations

with the three $[M]_0$ investigated and the experimental data for $[M]_0 = 4$ wt%. It can be seen that there is good agreement between experimental and calculated data for the conversion interval studied. Inasmuch as $[M]_0$ varied between 2 and 4% in the simulations, the copolymer composition was not very sensitive to the initial monomer mixture content.

Figure 7 shows the average number of radicals per particle ($\tilde{n}$, defined for zero-one kinetics as the ratio of the number of active particles/total number of particles) calculated with the modified simulation model for the 85:15 wt/wt of VAc/BuA ratio, this behavior is similar to that reported for emulsion polymerization [19]. The inset in Fig. 7 shows the results of simulations for the calculation of the average number of radicals per particle, at low conversions for different monomer compositions in the initial charge. It can be seen that the higher the BuA content, the higher the average number of radicals per particle.

Discussions

Compared with other polymerization processes (bulk, solution, or suspension) microemulsion copolymerization is a more complicated system. Polymerization rate is determined by a number of simultaneous events, among them, monomer partitioning between the phases, particle nucleation, adsorption, and desorption of radicals [20]. Particle stability is affected by the amount and type of surfactant and pH of the dispersing medium. In the present study, each component of the mixture of surfactants employed plays a different stabilization role: the anionic surfactant

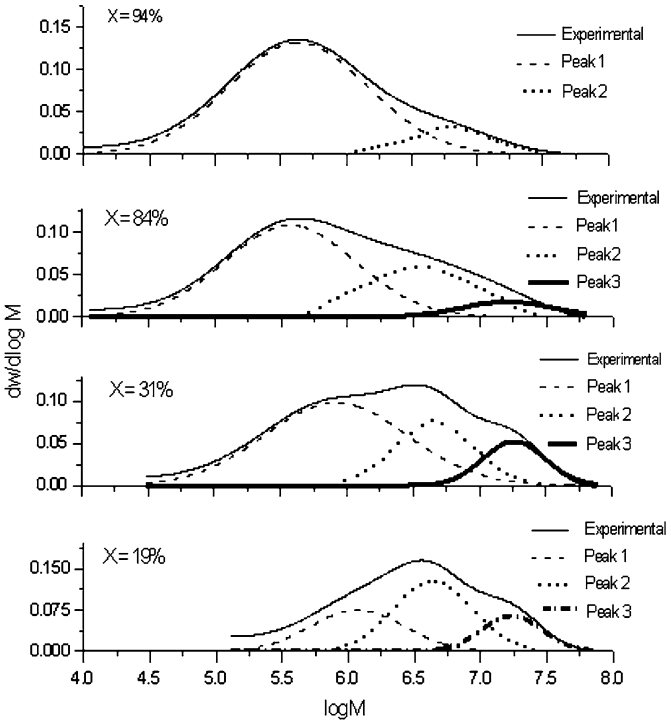

Fig. 5 Experimental molecular weight distributions and deconvolutions for different conversions in the batch microemulsion copolymerization of VAc:BuA (85:15 wt/wt) at 60 °C, 2 wt% of KPS with respect to the monomers content and 4 wt% of monomers mixture in the initial charge

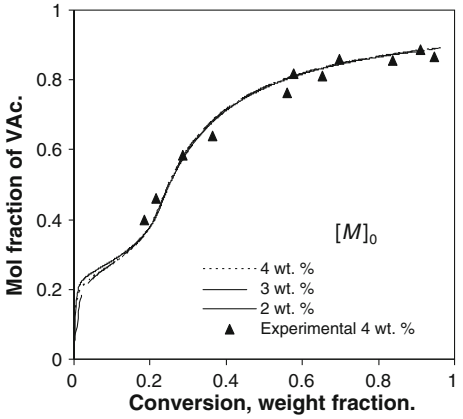

Fig. 6 Experimental and simulated cumulative copolymer composition of batch microemulsion copolymerization of VAc:BuA (85:15 wt/wt) at different $[M]_0$

stabilizes the polymer particles by electrostatic effects whereas the non-ionic surfactant (Brij-35) stabilizes the particles by steric effects. During reaction, pH shifts from an initial value close to 7.0–4.0 at the end of the copolymerization due to initiator decomposition [12]. The electrostatic effects in the microemulsion

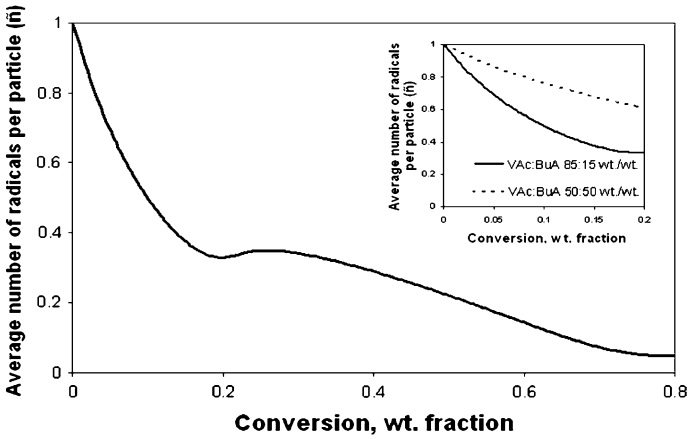

Fig. 7 Average number of radicals per particle throughout the batch microemulsion copolymerization of VAc:BuA (85:15 wt/wt) at 60 °C, 2 wt% of KPS with respect to the monomers content and 4 wt% of monomers mixture in the initial charge determined from simulation. *Inset* different monomers compositions in the initial charge (50:50 and 85:15 wt/wt at low conversions)

polymerization of vinyl acetate using AOT as the surfactant were studied by Sosa et al. [12], and found that the pH of the reacting medium influences the efficiency of KPS to initiate the reaction but it has no effect on 2,2′-Azobis(2-methylpropionamidine) dihydrochloride (V-50) efficiency. Furthermore, at neutral pH, faster reaction rates and higher conversions are achieved with KPS than with V-50 due to the different electrostatic interactions of free radicals with the negatively charged microemulsion droplets and polymer particles. These facts influence the dependence of the rate of polymerization as a function of the initial monomers concentration. From a logarithmic plot of maximum polymerization rate (not shown here), $R_{p_{max}}$, vs. initial monomers mixture concentration it was found that $R_{p_{max}}$ is proportional to $[M]_0^{1.26}$, which is different to the result reported by Torres-Plata [14] who found $R_{p_{max}} \propto [M]_0^{1.65}$ using V-50 (2,2′-azobis[2-amidinopropane] 2HCl) as initiator and AOT as surfactant (anionic) for the same VAc/BuA ratio. The electrostatic cage effect is operative in the Torres-Plata reacting system; that is, positively charged primary and/or oligomeric radicals are attracted to the negatively charged particles interface and trapped there reducing their efficiency to initiate the reaction. By contrast, the negatively charged KPS [21] free radicals are repelled by the droplets into the aqueous phase where they can react with the monomer dissolved there. These oligomeric radicals can grow up to a critical size and enter microemulsion droplets and existing particles or can be stabilized by recruiting surfactant and grow to become particles. Further, at 60 °C V-50 decomposes, independently of pH, ten times faster than KPS generating a higher radical flux ($k_{dV\text{-}50} = 3.2 \times 10^{-5}$ s^{-1}, $k_{dKPS} = 3.1 \times 10^{-6}$ s^{-1} [12]) whereas KPS decomposes at different rates as pH changes with a maximum at a pH of 7 [22]. Thus, the change of initiator and stabilizing agent changes the environment surrounding the polymerization loci and results in different dependencies of $R_{p_{max}}$ with the monomer mixture concentration.

Model simulations gave satisfactory fits for conversion (Fig. 2), particle diameters (Fig. 3), number density of particles (Fig. 4), and copolymer composition (Fig. 6) assuming micellar and homogeneous nucleation. Micellar nucleation occurs when an oligomeric radical in the aqueous phase is captured by a monomer swollen micelle (microemulsion droplets); in homogeneous nucleation, a radical in the aqueous phase reaches a critical size and precipitates, and it is stabilized with free surfactant forming a new particle.

The kinetics of microemulsion polymerization have much in common with that of emulsion polymerization, the most similar characteristic feature is the compartmentalization, where the radicals growing inside the particles are separated from each other, suppressing termination to a high extent and, as a consequence, high rates of polymerization and high molecular weights are obtained. In this work, the effect of monomers content on the kinetics of the copolymerization reaction was studied. When the initial monomer concentration increases, due to water-particle monomer equilibrium, higher monomer concentration should be present inside the particles giving as a result faster reaction rates. The values of the average number of radicals per particle predicted by the model decrease with conversion (Fig. 7) and with the VAc content (inset in Fig. 7), which is consistent with the experimental reports for VAc and BuA microemulsion and emulsion homopolymerizations [23, 24]. In the polymerization of VAc, it has been reported that monomer transfer reactions occur [24] leading to very low $\tilde{n}$ values because monomeric radicals desorb to the water phase due to their hydrophilicity. This $\tilde{n}$ behavior is similar to that reported in the literature [19]. At low conversions, monomeric radicals generated by chain transfer to monomer inside the polymer particles are mainly BuA-type (hydrophobic), therefore, a lower number of radicals are desorbed from the particles. However, as the BuA is depleted, more hydrophilic radicals (VAc-type) are formed by chain transfer to monomer which can leave the particles before adding monomer to initiate a new chain. The increase of the polymerization rate when most of the BuA has been depleted was explained by Delgado [25] and by Kong et al. [19] by the higher value of the propagation rate constant for VAc monomer compared to that for BuA ($k_{\mathrm{pVAc}} = 4000$ L mol^{-1} s^{-1}; $k_{\mathrm{pBuA}} = 200$ L mol^{-1} s^{-1}).

The small decrease of the average particle size at conversions between 25 and 30% (Fig. 3) implies that more particles are being nucleated. In a previous section, mention was made to the high water solubility of VAc which favors homogeneous nucleation during polymerization. Before the BuA is depleted, the less hydrophilic radicals generated by chain transfer to BuA do not escape to the aqueous phase, however, when BuA in the particles practically disappear, only VAc radicals are generated by chain transfer to monomer and some of them can escape to the aqueous phase, increasing the radical concentration there and giving as a result, a larger amount of particles formed by homogeneous particle nucleation, which is reflected by the model (Fig. 4).

It was found that the size of polymer particles increased with monomer concentration. The fact that the same surfactant concentration was used in the three polymerization conditions reported here implies that the higher the monomer concentration the higher the micelles swelling ($V_{\mathrm{org.}}$), as can be seen in Table 2.

Table 2 Initial volume fractions of each component in microemulsions calculated from thermodynamic equilibrium for different $[M]_0$

$[M]_0$ (wt%)	2	3	4
ϕ_{VAc} org.	0.45	0.62	0.71
ϕ_{BuA} org.	0.55	0.38	0.29
ϕ_{VAc} aq.	1.7×10^{-2}	2.1×10^{-2}	2.3×10^{-2}
ϕ_{BuA} aq.	7.0×10^{-4}	4.0×10^{-4}	2.0×10^{-4}
ϕ_{Water} aq.	0.982	0.980	0.977
$V_{org.}$ (cm^3)	0.748	1.83	3.31
$V_{aq.}$ (cm^3)	144.11	145.36	146.31

org. organic phase composed by BuA and VAc, *aq.* aqueous phase composed by solubilized VAc and BuA + water

Table 3 Final characteristics of copolymer latex obtained for different $[M]_0$

$[M]_0$ wt%	Conversion (wt%)	$M_w \times 10^{-6}$ (g/mol)	PDI[a]	D_p (nm)		N_p/cm^3 of water $\times 10^{-14}$	
				Exp.[b]	Sim.[c]	Exp.[b]	Sim.[c]
2	80.7	1.8	7.3	33	30	7.9	11.2
3	91.7	2.0	11.9	38	38	8.8	9.0
4	94.2	1.7	9.0	43	42	8.6	8.9

[a] Polydispersity index, [b] experimental, [c] simulation

Then, there is more monomer that can be transferred from the micelles to the particles causing larger particle size. Due to the high water solubility of VAc, homogeneous particle formation throughout the reaction will produce a relatively broad particle size distribution.

Figure 6 shows that there is a marked drift on copolymer composition throughout the reaction and that the copolymer becomes richer in PVAc with conversion. The initial copolymer composition is much richer in BuA due to the preference of the BuA to react with itself ($r_{BuA} = 6.2$) and because the VAc tends to react with BuA ($r_{VAc} = 0.028$) [20], and when the BuA is consumed the copolymer becomes richer in VAc.

Table 3 shows the final characteristics of the copolymer latex obtained for different initial monomers concentrations. It can be seen that M_w is not a function of monomer concentration and that polydispersity indices are greater than those reported in other microemulsion systems [18, 24, 26]. The MWD's (Fig. 5) are broad and at least two shoulders are present. The displacements of the MWD's to low molecular weights at high conversions indicate the formation of a new population of macromolecules. Because initially chains formed are richer in BuA (BuA has a chain transfer constant of $k_{tmBB}/k_{pBB} = 6.6 \times 10^{-5}$ [27]), Fig. 5, higher molecular weights are obtained. At high conversions, when copolymer chains become richer in VAc, the probability of chain transfer to VAc monomer is higher

($k_{tmAA}/k_{pAA} = 1.75 \times 10^{-4}$ to 2.25×10^{-4} [17]) resulting in shorter polymer chains.

From deconvolution analysis of the MWD results (Fig. 5), at low conversions three peaks can be observed and two peaks at final conversion. Peak 3 corresponds to chains richer in BuA; peak 2 corresponds to chains containing appreciable amounts of both monomers and peak 1 to chains richer in VAc. The proportion of high molecular weight population decreases as conversion increases (peak 3) because only chains richer in both monomers and in VAc are formed.

Conclusions

The partial phase diagram of the VAc:BuA/H_2O/SDS:Brij-35 shows an o/w microemulsion region slightly wider than the VAc:BuA/H_2O/SDS:AOT system. Micellar aggregation, solubilization, and interaction between emulsifiers and monomers are interrelated in a complex way which results in a broader o/w microemulsion region when Brij-35 replaces AOT as stabilizer. Monomer partitioning in microemulsion copolymerization systems has an important effect on the kinetics and particle nucleation when one or both monomers present relatively high water solubility. It was found that the initial monomers mixture concentration affects $R_{P_{max}}$ with a power of 1.26 which reflects the complex interactions of the reacting entities during the copolymerization.

It was found that particle size is a function of the initial monomers mixture concentration for a constant surfactant concentration. Latexes with average $D_p < 50$ nm were obtained.

The modified mathematical model with a minimum of adjustable parameters simulated adequately the microemulsion copolymerization of the VAc/BuA system. The model predicts homogeneous nucleation throughout most of the reaction due to the high water solubility of VAc. Good agreement between experimental and model predictions for conversion, copolymer composition, particle size and particle number versus time data was observed.

Acknowledgments Author Ovando-Medina acknowledges a scholarship (165731) from CONACyT Mexico and UASLP C08-FAI-04-5.9. This research was partially supported by CONACyT (Grant CB-61345).

Appendix

The mathematical model reported by Ovando-Medina et al. [11] to simulate microemulsion copolymerization was modified replacing the adjustable parameters by correlations to calculate kinetics and transport parameters. The main feature of the model includes micellar and homogeneous nucleation and thermodynamic equilibrium for the calculation of monomer partitioning between the phases.

Radical capture by micelles and particles

Radical capture was assumed to occur by diffusion. The rate coefficient for radical capture by micelles and particles is given by [28]:

$$k_{\mathrm{cm}i} = 4\pi\, r_{\mathrm{m}} F_j D_{\mathrm{w}i} N_{Av}$$
$$k_{\mathrm{cp}i} = 4\pi\, r_{\mathrm{p}} F_j D_{\mathrm{w}i} N_{Av}$$

where $k_{\mathrm{cm}i}$ and $k_{\mathrm{cp}i}$ are rate coefficients for type i radical capture by micelles and particles, respectively. F_j is the radical capture efficiency, r_{p} and r_{m} the radius of polymer particles and micelles, respectively, and D_{w} the diffusion coefficient of the radicals in the aqueous phase, N_{Av} is Avogadro's number. F_j remains as an adjustable parameter; this parameter accounts for all resistances to radical entry other than diffusion. The value used in the simulations for F_j was 1×10^{-5} which fitted well the experimental results and is in agreement with values reported in the literature [29].

Radical desorption from particles

Individual desorption coefficients were calculated as the rate of chain transfer to monomer and the probability of desorption of a single unit free radical [28]:

$$k_{\mathrm{d}i} = \frac{(k_{\mathrm{tmA}i} P_{\mathrm{A}}^{\mathrm{p}} + k_{\mathrm{tmB}i} P_{\mathrm{B}}^{\mathrm{p}}) M_{i\mathrm{p}} (2D_{\mathrm{p}}/r_{\mathrm{p}}^2)}{(2D_{\mathrm{p}}/r_{\mathrm{p}}^2 + k_{\mathrm{p}i\mathrm{A}} M_{\mathrm{Ap}} + k_{\mathrm{p}i\mathrm{B}} M_{\mathrm{Bp}})}$$

where $k_{\mathrm{tm}ij}$ is monomer chain transfer rate coefficient, D_{p} is the diffusion coefficient of radicals in polymer particles, $M_{i\mathrm{p}}$ are the concentrations of monomers A and B in the polymer particles, respectively, and $P_{\mathrm{A}}^{\mathrm{p}}$ and $P_{\mathrm{B}}^{\mathrm{p}}$ is the time-averaged probability of finding a free radical with ultimate type A and B unit, respectively, in the polymer particles phase [30] and is given by:

$$P_{\mathrm{A}}^{\mathrm{p}} = \frac{k_{\mathrm{pBA}} M_{\mathrm{Ap}}}{k_{\mathrm{pBA}} M_{\mathrm{Ap}} + k_{\mathrm{pAB}} M_{\mathrm{Bp}}}$$

and $P_{\mathrm{B}}^{\mathrm{p}} = 1 - P_{\mathrm{A}}^{\mathrm{p}}$.

References

1. Candau F (1992) Polymerization in media. In: Paleos CM (ed) Polymerization in organized media. Gordon and Breach Sci. Publ, Philadelphia, pp 215–283
2. Antonietti M, Basten R, Lohman S (1995) Polymerization in microemulsions: a new approach to ultrafine, highly functionalized polymer dispersions. Macromol Chem Phys 196:441–466
3. Xu XJ, Chew CH, Siow KS, Wong MK, Gan LM (1999) Microemulsion polymerization of styrene for obtaining high ratios of polystyrene/surfactant. Langmuir 15:8067–8071
4. Aguiar A, González-Villegas S, Rabelero M, Mendizábal E, Puig JE, Domínguez JM, Katime I (1999) Core–shell polymers with improved mechanical properties prepared by microemulsion polymerization. Macromolecules 32:6767–6771

5. Rabelero M, Zacarias M, Mendizabal E, Puig JE, Dominguez JM (1997) High-content polystyrene latex by microemulsion polymerization. Polym Bull 38:695–700
6. Ming W, Jones FN, Fu S (1998) Synthesis of nanosize poly(methyl methacrylate) microlatexes with high polymer content by a modified microemulsion polymerization. Polym Bull 40:749–756
7. Treviño ME, López RG, Peralta RD, Becerra F, Mendizábal E, Puig JE (1999) Polymerization of vinyl acetate in microemulsions stabilized with a mixture of dodecyltrimethylammonium bromide and didodecyldimethylammonium bromide. Polym Bull 42:411–417
8. Wu XQ, Schork FJ (2000) Batch and semibatch mini/macroemulsion copolymerization of vinyl acetate and comonomers. Ind Eng Chem Res 39:2855–2865
9. Herrera JR, Peralta RD, López RG, Cesteros LC, Mendizábal E, Puig JE (2003) Cosurfactant effects on the polymerization of vinyl acetate in anionic microemulsion media. Polymer 44:1795–1802
10. Pavel FM (2004) Microemulsion polymerization. J Disp Sci Tech 25:1–16
11. Ovando-Medina VM, Mendizábal E, Peralta RD (2005) Kinetics modeling of microemulsion copolymerization. Polym Bull 54:129–140
12. Sosa N, López RG, Peralta RD, Katime I, Becerra F, Mendizábal E, Puig JE (1999) Electrostatic effects on the polymerization of vinyl acetate in three-component anionic microemulsions. Macromol Chem Phys 200:2416–2420
13. Jovanovic R, Dubé MA (2001) Off-line monitoring of butyl acrylate and vinyl acetate homopolymerization and copolymerization in toluene. J Appl Polym Sci 82:2958–2977
14. Torres-Plata H (2001) Copolimerización en microemulsión del acetate de vinilo y del acrilato de butilo. Dissertation, Universidad Autónoma de Coahuila, México
15. Capek I (1999) On the free-radical microemulsion polymerization of butyl acrylate in the presence of poly(oxyethylene) macromonomer. Chem Papers 53:332–339
16. Donescu D, Fusulan L, Petcu C, Vasilescu M, Smarandache C, Capek I (2002) Ternary microemulsions of vinylic and acrylic monomers. Eur Polym J 38:1691–1701
17. Brandrup J, Immergut HE (1974) Polymer handbook, 2nd edn. Wiley, New York
18. Gómez-Cisneros M, López RG, Peralta RD, Cesteros LC, Katime I, Mendizábal E, Puig JE (2002) Polymerization of vinyl acetate in microemulsions stabilized with dodecyltrimethylammonium bromide and cetyltrimethylammonium bromide. Polymer 43:2993–2999
19. Kong XZ, Pichot C, Guillot J (1988) Kinetics of emulsion copolymerization of vinyl acetate with butyl acrylate. Eur Polym J 24:485–492
20. Ovando-Medina VM, Martínez-Gutiérrez H, Mendizábal E, Corona MA, Peralta RD (2009) Reactivity ratios and monomer partitioning in the microemulsion copolymerization of vinyl acetate and butyl acrylate. J Appl Polym Sci 111:329–337
21. Friend JP, Alexander AE (1968) Effect of surfactants on the polymerization of acrylamide in aqueous solutions. J Polym Sci Polym Chem Ed 6:1833–1839
22. Adhikari MS, Sarkar S, Banerjee M, Konar RS (1987) Thermal decomposition of potassium persulfate in aqueous solution at 50 °C in the presence of ethyl acrylate. J Appl Polym Sci 34:109–125
23. Sajjadi S, Brooks BW (1999) Butyl acrylate batch emulsion polymerization in the presence of sodium lauryl sulphate and potassium persulphate. J Polym Sci Part A Polym Chem 37:3957–3972
24. Gómez-Cisneros M, Treviño ME, Peralta RD, Rabelero M, Mendizábal E, Puig JE, Cesteros C, López RG (2005) Surfactant concentration effects on the microemulsion polymerization of vinyl acetate. Polymer 46:2900–2907
25. Delgado J (1986) Miniemulsion copolymerization of vinyl acetate and n-butyl acrylate. Dissertation, Lehigh University
26. Sosa N, Zaragoza EA, López RG, Peralta RD, Becerra F, Mendizábal E, Puig JE (2000) Unusual free radical polymerization of vinyl acetate in anionic microemulsion media. Langmuir 16:3612–3619
27. Maeder S, Gilbert R (1998) Measurement of transfer constant for butyl acrylate free-radical polymerization. Macromolecules 31:4410–4418
28. Arzamendi G, Asúa JM (1989) Monomer addition policies for copolymer composition control in semicontinuous emulsion copolymerization. J Appl Polym Sci 38:2019–2036
29. Hansen FK, Ugelstad J (1978) Particle nucleation in emulsion polymerization. I. A theory for homogenous nucleation. J Polym Sci Polym Chem Ed 16:1953–1979
30. Forcada J, Asúa JM (1990) Modeling of unseeded emulsion copolymerization of styrene and methyl methacrylate. J Polym Sci Part A Polym Chem 28:987–1009